

## A study of impurities in poly-Si wafers prepared by a vacuum casting method

G.H. Lee\*, S. Aukkaravittayapun<sup>a,c</sup>, J.S. Shin<sup>b</sup>, Z.H. Lee<sup>b</sup> and K.S. Lim<sup>a</sup>

Nuclear Materials development team, Korea Atomic Energy Research Institute, 150 Dukjindong Yusonggu Daejeon 305-600, Korea

<sup>a</sup>Department of Electrical Engineering and Computer Science, Korea Advanced Institute of Science and Technology, 373-1 Gusongdong, Yusonggu, Daejeon 305-701, Korea

<sup>b</sup>Department of Materials Science and Engineering, Korea Advanced Institute of Science and Technology, 373-1 Gusongdong, Yusonggu, Daejeon 305-701, Korea

<sup>c</sup>National Metal and Materials Technology Center (MTEC), National Science and Technology Development Agency, 114 Paholyothin Rd., Klong 1, Klong Luang, Pathumthani 12120 Thailand

A vacuum casting method was attempted to produce cheap poly-Si wafers ready for solar cell fabrication without any cutting or slicing. However, the  $5 \times 5$  cm<sup>2</sup> lab scale cast poly-Si wafers contained high carrier concentrations, above  $3 \times 10^{17}$ /cm<sup>3</sup>, and crystalline defects like grain boundaries and gas porosity. We carried out a set of vacuum casting experiment in order to identify the main sources of impurities during vacuum casting and investigated the impurities in the cast poly-Si wafers. The efficiency of the test solar cells fabricated on the cast poly-Si wafers was below 1.0% whereas the efficiency of the solar cell fabricated on the wafer sliced from starting Si was 5.5%. The low efficiency of the test cells was attributed to high carrier concentrations and gas porosity inside the cast poly-Si wafer.

**Key words:** vacuum casting, polycrystalline silicon, solar cells, impurities, gas porosity.

### Introduction

In order to reduce the cost of crystalline silicon (Si) solar cells, one approach is to produce low cost polycrystalline Si for solar cells. Up until now, poly-Si wafers have been produced by cutting or slicing Si ribbon from ribbon growth [1] or Si block from conventional solidification casting [2]. However, cutting and slicing leads to extra cost and waste of materials. Our intention was to produce instant poly-Si wafers for solar cell production without any cutting or slicing by direct casting of Si into a desired dimension mold. Although this challenge has been tried [3-5], so far there are no commercialized wafers produced from such processes due to relatively low quality wafers. Our new vacuum casting method has been tried in an attempt to overcome this challenge [6]. Nevertheless, casting of Si into a narrow cavity mold (<0.5 mm) has two main obstacles. First was the casting condition to obtain sound castings in the narrow mold cavity and second was the low quality of cast poly-Si wafers that show a high impurity concentration and small grain sizes. The first obstacle has been overcome but the second one still remains and caused very low solar cell

efficiency (<1%) [7]. Therefore, in this study, we investigated the causes of low-quality cast poly-Si wafers, emphasizing on impurities and their sources, and also the effect of carrier concentration on solar cell efficiency. Moreover, gas porosity inside cast poly-Si wafers was also investigated.

### Experiments

After graphite molds and graphite crucibles were ultrasonically cleaned in distilled water and in extra pure acetone, they were dried at 150°C for 1 day. The starting Si (poly-Si) was also cleaned and dried using the same cleaning method. After drying, the mold surfaces were coated by sprayed BN powder and dried again at 150°C for 1 day. The crucible and mold were assembled together, surrounded by carbon fiber, which is a heat insulator, and loaded into the casting system shown in Fig. 1.

The casting chamber of the quartz tube was pumped to 75 cmHg below atmospheric pressure and purged with Ar gas. The crucible was heated by induction heating while the chamber still remained at the reduced pressure. When the crucible temperature reached 1200 °C, the chamber was filled with Ar gas to 40 cmHg below atmospheric pressure in order to reduce the vapor pressure of Si. The crucible temperature was stabilized between 1450-1460°C for 15 minutes and the mold temperature was kept at ~1280°C. After 15

\*Corresponding author:  
Tel : +82-42-868-8359  
Fax: +82-42-862-5496  
E-mail: ex-ghlee@kaeri.re.kr

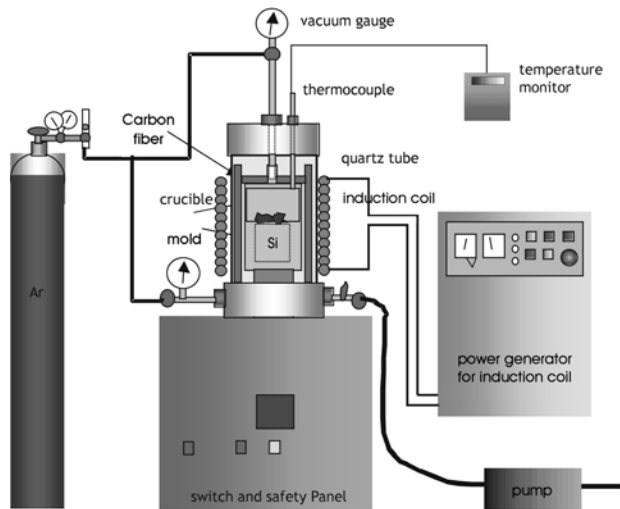


**Fig. 1.** A schematic diagram of vacuum casting system.

minutes, Ar gas was blown into the crucible above the molten Si. The Si melt was pressurized to flow into the mold underneath. The induction heating was then turned off and the system was let to cool down to room temperature with a cooling rate of  $\sim 2$  K/sec from 1450 °C to 1300 °C. This was our standard procedure for vacuum casting. The vacuum cast poly-Si wafers were characterized for surface appearance, microstructure and grain size by optical microscopy (OM). The resistivity ( $\rho$ ) and carrier concentration ( $N_c$ ) of the cast poly-Si wafers were measured by a Hall Van der Pauw system at room temperature. The impurities in the cast poly-Si wafers were analyzed by Fourier Transform Infrared Spectroscopy (FTIR) and Secondary Ion Mass Spectroscopy (SIMS).

Test solar cells were fabricated by using a simple  $n^+/p$  solar cell structure with a single  $\text{SiO}_2$  antireflection (AR) layer, excluding any high efficiency solar cell features such as hydrogen passivation, selective emitter, back surface field (BSF), surface texturing and contact annealing. All cast poly-Si wafers were mechanically polished down to a thickness of about 0.5 to 0.6 mm where they were too fragile to be further polished. The cast poly-Si wafers were then etched by isotropic poly-etchant ( $\text{HNO}_3:\text{H}_2\text{O}:\text{HF} = 10:4:1$ ) to obtain a thickness of  $\sim 0.3$  mm. The  $n^+/p$  junction was formed by thermal diffusion from a PDS<sup>®</sup> planar source at 950 °C for 30 minutes in a  $\text{N}_2$  atmosphere on top of an active area of 1  $\text{cm}^2$ . The emitter sheet resistance was about 15 to 20 Ohm/sq. The AR layer of  $\text{SiO}_2$  with a thickness of  $\sim 110$  nm was formed on the active area by oxidation at 850 °C. The AR layer was then patterned by photolithography for the front electrode. An aluminum (Al) film of 0.2 mm thick was deposited on the front and the back side of the solar cell. The front electrode was obtained by a lift-off process. The solar cell efficiencies of test cells were measured under air mass (AM) 1.5, 100  $\text{mW}/\text{cm}^2$

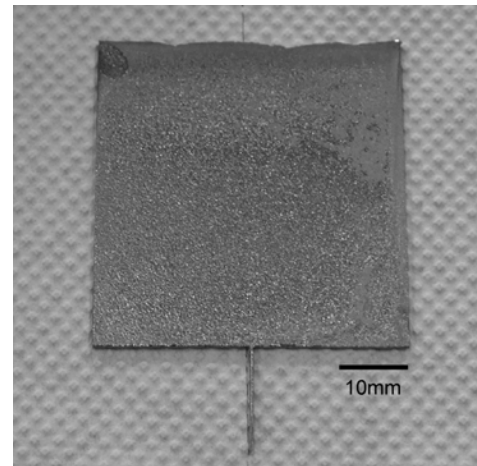


**Fig. 2.** As cast 1 mm thick and  $5 \times 5$   $\text{cm}^2$  sized poly-Si wafer with some BN coating powder remaining on its surface.

irradiation of a solar simulator (WXS-105H).

## Results and Discussion

A typical laboratory scale, cast poly-Si wafer of 5  $\text{cm} \times 5 \text{ cm} \times 1.0$  mm, obtained from vacuum casting is shown in Fig. 2. The thickness was aimed to be in the range of 0.25-0.3 mm, however, in this study we produced rather thicker wafers in order to study the impurities. The grain size was about 0.5 to 1 mm. In order to find out how much impurity was introduced into the cast poly-Si wafers during vacuum casting, we firstly checked the  $N_c$  of the starting Si, which is a semiconductor-grade poly-Si left in the quartz crucible after a CZ-process, by a Hall Van der Pauw system. The  $\rho$  and  $N_c$  of the starting Si are shown in Table 1. The starting Si was a p-type and thus  $N_c$  represented the hole concentration. Then we carried out three casting experiments using our standard casting procedure described above. The 1<sup>st</sup> casting used a new graphite crucible. For the 2<sup>nd</sup> and 3<sup>rd</sup> castings, the crucible was reused and there was no recharge of starting Si into the crucible. The  $\rho$  and  $N_c$  of these three cast poly-Si wafers are shown in Table 1 and they were all p-type Si. After the 1<sup>st</sup> casting, 2<sup>nd</sup> casting and 3<sup>rd</sup> casting, the  $N_c$  was increased from  $1.91 \times 10^{15} \text{ cm}^{-3}$  to  $3.49 \times 10^{17} \text{ cm}^{-3}$ , to  $1.19 \times 10^{18} \text{ cm}^{-3}$  and to  $1.25 \times 10^{18} \text{ cm}^{-3}$ , respectively. The additional  $N_c$  inevitably was from both the

**Table 1.** Resistivity ( $\rho$ ) and carrier concentration ( $N_c$ ) of Si at different steps

Materials	$\rho$ ( $\Omega\text{-cm}$ )	$N_c$ ( $\text{cm}^{-3}$ ) p-type	Added ( $\text{cm}^{-3}$ )
Starting Si	7.92	$1.91 \times 10^{15}$	-
Si in crucible	3.07	$1.13 \times 10^{16}$	$9.39 \times 10^{15}$
1 <sup>st</sup> casting	0.098	$3.49 \times 10^{17}$	$3.37 \times 10^{17}$
2 <sup>nd</sup> casting	0.034	$1.19 \times 10^{18}$	$8.41 \times 10^{17}$
3 <sup>rd</sup> casting	0.033	$1.25 \times 10^{18}$	$6.0 \times 10^{16}$

graphite crucible and/or the BN coated graphite mold. In order to know how much Nc was introduced by each of them, the same casting condition as for the 1<sup>st</sup> casting was used but the melt was solidified in the graphite crucible instead. The melt-solidified Si in the graphite crucible, that is Si in the crucible, was sliced and measured for Nc. The Nc (also p-type) of the Si in the crucible was  $1.13 \times 10^{16} \text{ cm}^{-3}$  as shown in Table 1.

From these data, we can deduce that, after heating for ~15 minutes at about 1450 to 1460°C in the graphite crucible, an additional Nc of  $9.39 \times 10^{15} \text{ cm}^{-3}$  (~5 times the initial value) was introduced from the graphite crucible. And for the 1<sup>st</sup> casting, an additional Nc of  $3.37 \times 10^{17} \text{ cm}^{-3}$  (~176 times the initial value) was added into the cast poly-Si wafer from the BN powder-coated mold. Obviously, the mold was ~36 times more effective than the crucible in term of its Nc contribution to the cast poly-Si wafer.

Nevertheless for the 2<sup>nd</sup> casting, the result was contradictory to the former case. We can assume that the mold effect on Nc should be the same since the mold was prepared in the same manner. Therefore, the higher Nc must be introduced by the crucible. This is reasonable because the longer heating time can give rise to impurity incorporation from the graphite crucible into the Si melt and then eventually the poly-Si wafer. Thus, in the case of the prolonged heating time, the crucible become more and more serious in terms of incorporation of impurities. The additional Nc of  $\sim 8.41 \times 10^{17} \text{ cm}^{-3}$  or ~2.5 times of that from the mold was introduced from the crucible. For the 3<sup>rd</sup> casting, however, Nc was just slightly higher than that of the 2<sup>nd</sup> casting. Probably, after the 2<sup>nd</sup> casting or after an accumulated heating time of ~30 minutes, the impurity incorporation from the crucible has more or less reached its maximum point.

FTIR analysis in Fig. 3 shows that after the Si was melted in the graphite crucible for 15 minutes, a substantial amount of Carbon (C) and Oxygen (O) have been introduced into the Si as seen from the stronger

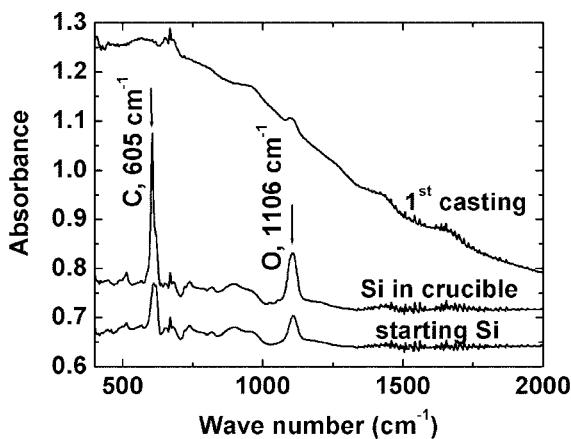


Fig. 3. FTIR spectrum of starting Si, Si in Crucible, and after 1<sup>st</sup> casting.

peaks from the Si in the crucible compared to the starting Si peaks at  $605 \text{ cm}^{-1}$  and  $1106 \text{ cm}^{-1}$ , respectively. However, there is no observation of a significant change at other absorption peaks due to other impurities such as Nitrogen (N), Hydrogen (H) or Boron (B). Since the infrared absorption coefficient due to an impurity in Si is proportional to the impurity concentration, this can be approximately estimated from the absorption coefficient of the Si-C absorption peak at  $605 \text{ cm}^{-1}$  that after heating in crucible for 15 minutes, the C content increased ~3-4 times of its initial value. Also from the absorption coefficient of the Si-O absorption peak at  $1106 \text{ cm}^{-1}$ , the O content increased ~2 times of its initial value. For the 1<sup>st</sup>, 2<sup>nd</sup> and 3<sup>rd</sup> castings, however, broad absorption spectra were obtained. This is because their resistivity was too low for FTIR analysis ( $<0.5 \text{ Ohm-cm}$  for p-type) and the absorption peaks due to the impurities in Si were dominated by free carrier absorption. The absorption curves for the 2<sup>nd</sup> and 3<sup>rd</sup> castings are not presented here because their absorbance was much higher than that for the 1<sup>st</sup> casting and there was almost no absorption peak observed at all. Nevertheless, this FTIR data confirms that Nc was greatly increased by the BN-coated mold after casting.

To investigate the impurities in cast poly-Si wafers, SIMS was performed on a poly-Si cast wafer which had an Nc of  $3.08 \times 10^{18} \text{ cm}^{-3}$  (p-type). The higher concentration was due to the re-use of the graphite crucible. The result of the SIMS analysis of the cast wafer is shown in Table 2. The B concentration was  $\sim 3\text{-}4 \times 10^{18} \text{ cm}^{-3}$  which is almost the same value as Nc. Since C, O, N and H in Si generally are not electrically active [8], therefore Nc was believed to represent the B concentration in the cast poly-Si wafers.

In Table 2, the C content is rather high ( $\sim 2\text{-}3 \times 10^{19} \text{ cm}^{-3}$ ), about 100 times higher than the solubility limit in solid Si ( $3.5 \times 10^{17} \text{ cm}^{-3}$ ). This higher C content was obtained even when a quartz crucible was inserted inside the graphite crucible and the Si melt was not indirect contact with the graphite crucible and graphite mold (due to the BN coating). Therefore, C incorporation into the Si may have taken place via  $\text{CO}_{(g)}$  inside the crucible during heating [9] and also possibly via Carbon dust (from the Carbon fiber used as heat insulator) flying into the crucible during the loading of the crucible/mold into the casting chamber. For the

Table 2. SIMS analysis at different depth from a surface of a 1 mm thick cast wafer using quartz crucible insert inside graphite crucible

Depth from surface (mm)	B ( $\text{cm}^{-3}$ )	C ( $\text{cm}^{-3}$ )	O ( $\text{cm}^{-3}$ )	H ( $\text{cm}^{-3}$ )
0.1	$3.3 \times 10^{18}$	$1.3 \times 10^{19}$	$2.0 \times 10^{16}$	$1.3 \times 10^{19}$
0.2	$4.0 \times 10^{18}$	$1.5 \times 10^{19}$	$1.0 \times 10^{16}$	$8.0 \times 10^{18}$
0.4	$4.4 \times 10^{18}$	$3.6 \times 10^{19}$	$4.0 \times 10^{16}$	$2.0 \times 10^{19}$

case without the quartz crucible, there will be direct contact of Si melt to the graphite crucible, thus an even higher C content can be expected. For O ( $\sim 1-4 \times 10^{16} \text{ cm}^{-3}$ ) and H ( $\sim 1-2 \times 10^{19} \text{ cm}^{-3}$ ), they may be incorporated into the Si at elevated temperature in the form of  $\text{H}_2\text{O}_{(g)}$ , outgasing from the residual moisture inside the (porous) graphite crucible and mold left after drying. For the N the content was unfortunately not investigated by SIMS but it was believed to have been approximately the same amount as that of B since BN will definitely introduce B and N at the same time into the cast poly-Si wafers.

Test solar cells were fabricated and the solar cell efficiency ( $\eta$ ) of the cast poly-Si wafers as well as the starting Si are shown in Table 3. The starting Si (A) showed an  $\eta$  of 5.5% while the vacuum cast poly-Si wafers B, C and D showed an  $\eta$  of less than 1.0%. We plot the efficiency versus carrier concentration of the test cells in Table 3. It seems that the  $\eta$  of the test cells decreases when increasing  $N_c$  as shown in Fig. 4. This is an usual case since minority carrier life time, related to solar cell efficiency, would decrease for a higher doping concentration and thus with a decrease of  $\eta$ . Therefore in order to improve  $\eta$ , it is very necessary to reduce the  $N_c$  of cast poly-Si wafers. In addition, from surface inspection of the test cells, we also found that the surface roughness of cast poly-Si wafers, B, C and D were very rough ( $\sim 1.5-3.0 \mu\text{m}$ ), compared to the thickness of the front electrode ( $0.2 \mu\text{m}$ ). The rough

**Table 3.** Carrier concentration ( $N_c$ ) and efficiency ( $\eta$ ) of test solar cells

Sample	$N_c \text{ (cm}^{-3}\text{)}$	$\eta \text{ (%)}$
Starting Si (A)	$1.91 \times 10^{15}$	5.5
1 mm (B)	$2.96 \times 10^{18}$	0.45
0.5 mm BN (C)	$4.49 \times 10^{17}$	0.90
0.5 mm C (D)	$3.72 \times 10^{18}$	0.10

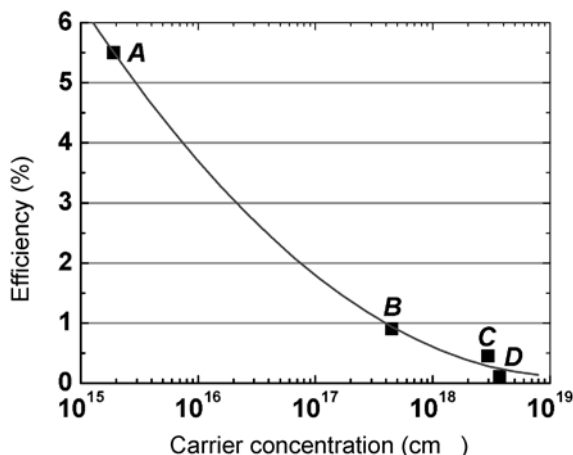


**Fig. 4.** The efficiency ( $\eta$ ) versus carrier concentration ( $N_c$ ) of test solar cells.

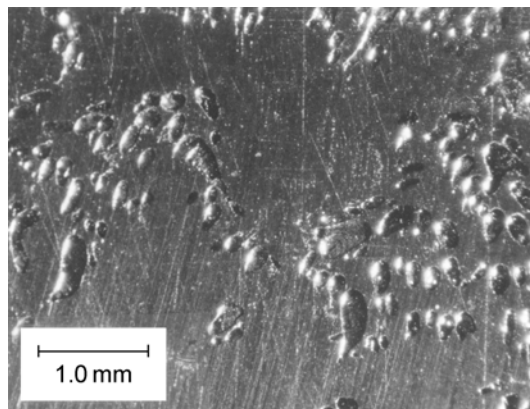


**Fig. 5.** OM image of the gas porosity at the half thickness of a cast poly-Si wafer.

surface, occurred after deep etching of wafers from 0.5-0.6 mm to 0.3 mm, and can lead to discontinuity of front electrode, thus lowering the current and  $\eta$ . If the front electrode is much thicker than the roughness, a higher  $\eta$  would be expected. Moreover, in the middle of the cast wafers B, C and D, gas porosity as shown in Fig. 5 was also observed. This gas porosity (voids) inside the solar cell can be the recombination centers inside the solar cell and it also would result in a low  $\eta$ .

## Conclusion

High  $N_c$  (hole) concentration in vacuum cast poly-Si wafers was due to the mold. However, with a longer heating time, more  $N_c$  was also added from the crucible. C in Si was increased enormously during heating in the graphite crucible while B and N were added into the Si from the BN coating (termed heavily doping material for Si casting). Thus, it is necessary to find a new coating material and reduce the heating time to reduce  $N_c$  and other impurities. The residual  $\text{H}_2\text{O}$  in the porous graphite mold and crucible was also believed to be the source for H and O. The  $\eta$  of the test cells decreased with increasing  $N_c$ . The gas porosity from saturated nitrogen ( $\text{N}_2$ ) inside the cast poly-Si wafers was also believed to suppress the  $\eta$ .

## Acknowledgments

This research was supported by Korea Science and Engineering Foundation (KOSEF) with Grant No. 1999-1-301-003-3 and also partly supported by the BK21-project of the Ministry of Education.

## References

1. R.L. Wallace, J.I. Hanoka, A. Rohatgi and G. Crotty, Sol. Energy Mater. Sol. Cells 48 (1997) 179-186.
2. T. Saito, A. Shimura and S. Ichikawa, in Proc. 15th IEEE PVSC, May 1981, edited by C.J. Bishop (IEEE PVSC,

- 1981) p. 576.
3. T.F. Ciszek, in "The capillary action shaping technique and its application" (Springer-Verlag, 1981) p. 109.
  4. M. Suzuki, I. Hide, T. Yokoyama, T. Matsuyama, Y. Hatanaka and Y. Maeda, *J. Crystal Growth* 104[1] (1990) 102-107.
  5. A. Beck, J. Geissler and D. Helmreich, *J. Crystal Growth* 104[1] (1990) 113-118.
  6. G.H. Lee and Z.H. Lee, *J. Crystal Growth* 233 (2001) 45-51.
  7. G.H. Lee and Z.H. Lee, *J. Korean Cryst. Growth & Cryst. Tech.* 12[3] (2002) 120-125.
  8. W.M. Bullis, in "Silicon Materials Properties, Handbook of Semiconductor Silicon Technology" (Noyes Publications, 1990) p. 364.
  9. W. Zulehner and D. Huber, in "Czochralski-Grown Silicon, Crystals Growth-Properties and Application Vol. 8: Silicon Chemical Etching", (Springer-Verlag, 1982) p. 17.